Int. J. Solids Structures Vol. 20, No. 2, pp. 107–120, 1984
Printed in Great Britain
0020-7683/84 $3.00 + .00

A FLUGGE-TYPE THEORY FOR THE ANALYSIS OF ANISOTROPIC LAMINATED NON-CIRCULAR CYLINDRICAL SHELLS

KOSTAS P. SOLDATOS
Department of Mechanics, University of Ioannina, Greece

(*Received* 31 *May* 1983)

Abstract—For a generally anisotropic laminated thin elastic non-circular cylindrical shell, subjected to a combined loading, the equations of motion of a second approximation Flugge-type theory are derived and expressed in terms of the shell middle-surface displacement components. As an application, for the free vibration problem of a cross-ply laminated non-circular cylindrical shell subjected to S2 simply supported edge boundary conditions, these equations are solved by employing the method of Galerkin. For a family of regular antisymmetric cross-ply laminated oval shells, numerical results are obtained and discussed. Comparisons are also made between some of the obtained results and corresponding results obtained from the solution of the quasi-shallow shell Donnell-type equations of motion.

1. INTRODUCTION

During the past two decades a considerable amount of attention has been concentrated in problems concerned with the investigation of the behaviour of laminated composite structures. Thus, for the stability and dynamic analysis of laminated composite thin elastic cylindrical shells, the equations of several type theories have been derived and used.

For generally anisotropic laminated circular cylindrical shells, Donnell's shallow shell theory[1] has been used for the equations derived by Dong *et al.*[2] in terms at the Airy's stress function and the normal to the shell middle surface displacement. The same type of equations, but in terms of the shell middle surface displacement components, can be obtained as a special case of those equations quoted by Soldatos in Ref.[3]. Love's first approximation shell theory[4] has been used for the sets of equations derived by Bert *et al.*[5] and by Greenberg and Stavsky[6]. Finally, Flugge's second approximation theory[7] has been used for the derivation of the corresponding equations presented by Cheng and Ho[8].

For laminated composite noncircular cylindrical shells, a set of Donnell-type equations has been recently presented by Soldatos and Tzivanidis[9]. However, Donnell-type equations are suitable only for the analysis of short cylindrical shells (see, e.g. Refs.[10], 11]). Furthermore, with the equations quoted in Ref.[9] only cross-ply laminated shells can be studied.

The main purpose of the present paper is to extend Flugge's theory to consideration of the dynamic behaviour and stability under combined loading of a generally anisotropic laminated noncircular cylindrical shell. A function of the shell circumferential coordinate is introduced to describe the divergence of the noncircular shell configuration from that of a corresponding circular one. Then, the Flugge-type equations are expressed in terms of this function as well as of the shell middle surface displacement components.

As an application of the derived equations, the free vibration problem of a cross-ply laminated noncircular cylindrical shell subjected to S2 simply supported edge boundary conditions (following Almroth's classification[12]) is introduced. It is solved by the procedure followed in Ref.[9], where the Donnell-type equations had been solved by employing the method of Galerkin. Then, for the case of a regular anisymmetric cross-ply laminated oval cylindrical shell, a comparison between corresponding results obtained by both Flugge and Donnell theories is attempted. Finally, some more numerical results obtained by Flugge's theory are presented and discussed.

2. CONSTITUTIVE EQUATIONS

Figure 1 indicates the nomenclature of the middle surface of a laminated thin noncircular cylindrical shell consisting of an arbitrary number of layers. Each individual layer is considered

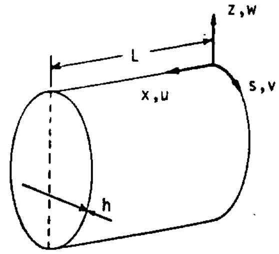

Fig. 1. Nomenclature of the non-circular cylindrical shell.

to behave macroscopically as a homogeneous, anisotropic, linearly elastic material. Furthermore, the layers are assumed to be perfectly bonded together.

Under these circumstances, each layer (say the kth one) is assumed to be in a state of plane stress governed by the two-dimensional Hooke's law,

$$\begin{bmatrix} \sigma_x^{(k)} \\ \sigma_s^{(k)} \\ \sigma_{xs}^{(k)} \end{bmatrix} = \begin{bmatrix} Q_{11}^{(k)} & Q_{12}^{(k)} & Q_{16}^{(k)} \\ Q_{12}^{(k)} & Q_{22}^{(k)} & Q_{26}^{(k)} \\ Q_{16}^{(k)} & Q_{26}^{(k)} & Q_{66}^{(k)} \end{bmatrix} \begin{bmatrix} \epsilon_x \\ \epsilon_s \\ \epsilon_{xs} \end{bmatrix}, \tag{1}$$

where, for the Flugge's theory used here, the shell strain components can be expressed, in terms of the middle surface displacement components, as follows[7]:

$$\begin{aligned} \epsilon_x &= u_{,x} - zw_{,xx},\ \epsilon_s = v_{,s} - z(1+z/R)^{-1}w_{,ss} + w(R+z)^{-1}, \\ \epsilon_{xs} &= u_{,s}(1+z/R)^{-1} + v_{,x}(1+z/R) - zw_{,xs}[1+(1+z/R)^{-1}]. \end{aligned} \tag{2}$$

It is convenient to adopt here the expression

$$(1/R) = (1/R_0)f(s), \tag{3}$$

used in Ref.[9], for the shell middle surface variable radius of curvature. In eqn (3), R_0 is a constant and $f(s)$ is a function of the circumferential co-ordinate s, so that for $f(s) = 1$ the configuration of the shell middle surface is that of a circular cylinder of radius R_0. Thus, $f(s)$ can be considered as a function describing the divergence of the configuration of the noncircular shell from that of a corresponding circular cylindrical one, both of them having the same circumferential length ($2\pi R_0$).

The well known force and moment resultants are, respectively, defined as follows:

$$\begin{aligned} \mathbf{N}^T &= [N_x, N_s, N_{xs}, N_{sx}] = \int_{-h/2}^{h/2} [\sigma_x(1+z/R), \sigma_s, \sigma_{xs}(1+z/R), \sigma_{xs}]\,\mathrm{d}z, \\ \mathbf{M}^T &= [M_x, M_s, M_{xs}, M_{sx}] = \int_{-h/2}^{h/2} [\sigma_x(1+z/R), \sigma_s, \sigma_{xs}(1+z/R), \sigma_{xz}]\,\mathrm{d}z \end{aligned} \tag{4}$$

where h is the shell constant thickness. Using, where it is needed, the approximation

$$(1+z/R)^{-1} = 1 - z/R + z^2/R^2 + 0(z^3/R^3), \tag{5}$$

and carrying out the noted integrations, the following constitutive equations are obtained,

$$\begin{bmatrix} \mathbf{N} \\ \mathbf{M} \end{bmatrix} = \begin{bmatrix} \mathbf{A}' & \mathbf{B}' \\ \mathbf{C}' & \mathbf{D} \end{bmatrix} \begin{bmatrix} \mathbf{e} \\ \mathbf{k} \end{bmatrix}, \tag{6}$$

where the components of the vectors $\mathbf{e}$ and $\mathbf{k}$ represent the strains and the changes of curvature, respectively, of the middle surface given as follows,

$$e_x = u_{,x}, e_s = v_{,s} + z/R, e_{xs} = u_{,s} + v_{,x},$$
$$k_x = - w_{,xx}, k_s = -(w_{,ss} + z/R^2), k_{xs} = -2w_{,xs} + (v_{,x} - u_{,s})/R. \quad (7)$$

The components of the stiffness submatrices $\mathbf{A}'$, $\mathbf{B}'$, and $\mathbf{C}'$ are given in terms of the components of the well known extensional, coupling and bending submatrices[13],

$$(A_{ij}, B_{ij}, D_{ij}) = \int_{-h/2}^{h/2} Q_{ij}(1, z, z^2)\,dz, \quad i, j = 1, 2, 6 \quad (8)$$

in Appendix A.

The coupling stiffness B_{ij} represent the shell lamination effect which is an additional coupling between bending and extension, except that coupling due to the nonzero shell curvature. For homogeneous shells all B_{ij} become equal to zero, so that this additional coupling disappears. It must be noted here that in the case of a first approximation shell theory the elements of both matrices $\mathbf{B}'$ and $\mathbf{C}'$ coincide with the coupling stiffness B_{ij} (see, e.g. Ref.[5]).

3. EQUATIONS OF MOTION

Flugge's differential equations for vibration and buckling under combined loading can be expressed in terms of the shell force and moment resultants, as follows[7]:

$$N_{x,x} + N_{sx,s} - pR(u_{,ss} - w_{,x}/R) - Pu_{,xx} - 2Tu_{,xs} = \rho_0 u_{,tt}$$
$$N_{s,s} + N_{xs,x} + (M_{s,s} + M_{xs,x})/R - pR(v_{,ss} + w_{,s}/R) - Pv_{,xx} - 2T(v_{,xs} + w_{,x}/R) = \rho_0 v_{,tt}$$
$$-N_s/R + M_{x,xx} + (M_{xs} + M_{sx})_{,xs} + M_{s,ss} - pR[w_{,ss} + (u_{,x} - v_{,s}/R] - Pw_{,xx} + 2T(v_{,x}/R - w_{,xs}) = \rho_0 w_{,tt}, \quad (9)$$

where p is the initial external radial pressure, P and T are the initial axial compression and torsional force per unit length, respectively, t is time and the inertia factor ρ_0 is defined as

$$\rho_0 = \int_{-h/2}^{h/2} \rho\,dz, \quad (10)$$

ρ being the shell mass density varying, in general, from layer to layer.

Using nondimensional coordinates,

$$\eta = x/L, \xi = s/2\pi R_0, \quad 0 \le \eta, \xi \le 1, \quad (11)$$

and introducing the nondimensional parameters,

$$\lambda = R_0/L, (\bar{p}, \bar{P}, \bar{T}, \bar{\rho}) = (pR_0, P, T, \rho_0 R_0^2)/A_{11},$$
$$(\bar{A}_{ij}, \bar{B}_{ij}, \bar{D}_{ij}) = (A_{ij}, B_{ij}/R_0, D_{ij}/R_0^2)/A_{11}, \quad (12)$$

eqns (9) can be expressed, in terms of the shell middle surface displacement components, as follows

$$\begin{bmatrix} L_{11} & L_{12} & L_{13} \\ L_{21} & L_{22} & L_{23} \\ L_{31} & L_{32} & L_{33} \end{bmatrix} \begin{bmatrix} u \\ v \\ w \end{bmatrix} = [0], \quad (13)$$

where $L_{ij}(i, j = 1, 2, 3)$ are the following linear partial differential operators:

$$L_{11} = (2\pi\lambda)^2(1 + \bar{B}_{11}f - \bar{P})(\ )_{,\eta\eta} + 4\pi\lambda(\bar{A}_{16} - \bar{T})(\ )_{,\eta\xi}$$
$$+ [(\bar{A}_{66} - \bar{B}_{66}f + \bar{D}_{66}f^2)(\ )_{,\xi}]_{,\xi} - (\bar{p}/f)(\ )_{,\xi\xi} - 4\pi^2\bar{\rho}(\ )_{,tt},$$
$$L_{12} = (2\pi\lambda)^2(\bar{A}_{16} + 2\bar{B}_{16}f + \bar{D}_{16}f^2)(\ )_{,\eta\eta} + \bar{A}_{26}(\ )_{,\xi\xi}$$
$$+ 2\pi\lambda(\bar{A}_{12} + \bar{A}_{66} + \bar{B}_{12}f)(\ )_{,\eta\xi} + 2\pi\lambda[f(\ )_{,\eta}]_{,\xi},$$

$$
\begin{aligned}
L_{13} = {} & 4\pi^2\lambda(\bar{A}_{12}f+\bar{p})(\,)_{,\eta} + 2\pi[(\bar{A}_{26}f-\bar{B}_{26}f^2+\bar{D}_{26}f^3)(\,)]_{,\xi} \\
& -4\pi^2\lambda^3(\bar{B}_{11}+\bar{D}_{11}f)(\;)_{,\eta\eta\eta} - 2\pi\lambda^2(3\bar{B}_{16}+\bar{D}_{16}f)(\;)_{,\eta\eta\xi} \\
& -\lambda(\bar{B}_{16}+2\bar{B}_{66})(\;)_{,\eta\xi\xi} - \lambda\bar{D}_{66}[f(\;)_{,\eta\xi}]_{,\xi} - (1/2\pi)\bar{B}_{26}(\;)_{,\xi\xi\xi} - (1/2\pi)\bar{D}_{26}[f(\;)_{,\xi\xi}]_{,\xi}, \\
L_{21} = {} & (\bar{B}_{26}-\bar{D}_{26}f)f'(\;)_{,\xi} + (2\pi\lambda)^2[\bar{A}_{16}+2\bar{B}_{16}f+\bar{D}_{16}f^2](\;)_{,\eta\eta} \\
& +2\pi\lambda[\bar{A}_{12}+\bar{A}_{66}+(\bar{B}_{12}+\bar{B}_{66})f](\;)_{,\eta\xi} + \bar{A}_{26}(\;)_{,\xi\xi}, \\
L_{22} = {} & 2\pi\lambda(\bar{B}_{26}+\bar{D}_{26}f)f'(\;)_{,\eta} + (2\pi\lambda)^2(\bar{A}_{66}+3\bar{B}_{66}f+3\bar{D}_{66}f^2-\bar{P})(\;)_{,\eta\eta} \\
& +4\pi\lambda(\bar{A}_{26}+2\bar{B}_{26}f+\bar{D}_{26}f^2-\bar{T})(\;)_{,\eta\xi} + [\bar{A}_{22}+\bar{B}_{22}f-\bar{p}/f](\;)_{,\xi\xi} - 4\pi^2\bar{\rho}(\;)_{,tt}, \\
L_{23} = {} & 4\pi^2\lambda(\bar{A}_{26}+\bar{B}_{26}f-2T)f(\;)_{,\eta} + 2\pi(\bar{A}_{22}-\bar{B}_{22}f')[f(\;)]_{,\xi} \\
& +2\pi\bar{D}_{22}f'[f^2(\;)]_{,\xi} - 2\pi\bar{p}(\;)_{,\xi} - 4\pi^2\lambda(\bar{A}_{26}+\bar{B}_{26}f+2\bar{T})f(\;)_{,\eta} \\
& -\lambda\bar{D}_{26}f'(\;)]_{,\eta\xi} - 4\pi^2\lambda^3(\bar{B}_{16}+2\bar{D}_{16}f(\;)_{,\eta\eta\eta} - 2\pi\lambda^2[\bar{B}_{12}+2\bar{B}_{66} \\
& +(\bar{D}_{12}+3\bar{D}_{66})f](\;)_{,\eta\eta\xi} - \lambda(3\bar{B}_{26}+2\bar{D}_{26}f)(\;)_{,\eta\xi\xi} - (1/2\pi)(\bar{B}_{22}-\bar{D}_{22}f')(\,)_{,\xi\xi\xi}, \\
L_{31} = {} & 4\pi^2\lambda(\bar{A}_{12}f+\bar{p})(\;)_{,\eta} + 2\pi(\bar{A}_{26}-\bar{B}_{26}f+\bar{D}_{26}f^2)f(\;)_{,\xi} - 4\pi^2\lambda^3(\bar{B}_{11}+\bar{D}_{11}f)(\;)_{,\eta\eta\eta} \\
& -6\pi\lambda^2\bar{B}_{16}(\;)_{,\eta\eta\xi} - 2\pi\lambda^2\bar{D}_{16}[f(\;)_{,\eta\eta}]_{,\xi} - \lambda(\bar{B}_{12}+2\bar{B}_{66})(\;)_{,\eta\xi\xi} - \lambda\bar{D}_{66}[f(\;)_{,\eta\xi}]_{,\xi} \\
& -(1/2\pi)\bar{B}_{26}(\;)_{,\xi\xi\xi} + (1/2\pi)\bar{D}_{26}[f(\;)_{,\xi}]_{,\xi\xi}, \\
L_{32} = {} & 4\pi^2\lambda(\bar{A}_{26}+\bar{B}_{26}f-2\bar{T})f(\;)_{,\eta} + 2\pi(\bar{A}_{22}f-\bar{p})(\;)_{,\xi} - 4\pi^2\lambda^3(\bar{B}_{16}+2\bar{D}_{16}f)(\;)_{,\eta\eta\eta} \\
& -2\pi\lambda^2[\bar{B}_{12}+2\bar{B}_{66}+(\bar{D}_{12}+3\bar{D}_{66})f](\;)_{,\eta\eta\xi} \\
& -3\lambda\bar{B}_{26}(\;)_{,\eta\xi\xi} - \lambda\bar{D}_{26}[2f(\;)_{,\eta\xi}+f'(\;)_{,\eta}]_{,\xi} - (1/2\pi)\bar{B}_{22}(\;)_{,\xi\xi\xi}, \\
L_{33} = {} & 4\pi^2(\bar{A}_{22}\bar{B}_{22}f+\bar{D}_{22}f^2)f^2(\,) - 4\pi\lambda(\bar{B}_{26}-\bar{D}_{26}f)f'(\,)_{,\eta} \\
& -(2\pi\lambda)^2(2\bar{B}_{12}f-\bar{P})(\;)_{,\eta\eta} - 4\pi\lambda(2\bar{B}_{26}f-\bar{D}_{26}f^2-\bar{T})(\;)_{,\eta\xi} \\
& -[\bar{B}_{22}f-\bar{D}_{22}f^2-\bar{p}/f](\;)_{,\xi\xi} - [(\bar{B}_{22}f-\bar{D}_{22}f^2(\;)]_{,\xi\xi} \\
& +8\pi\lambda^3\bar{D}_{16}(\;)_{,\eta\eta\eta\xi} + (2\lambda/\pi)\bar{D}_{26}(\;)_{,\eta\xi\xi\xi} + 4\pi^2\lambda^4\bar{D}_{11}(\;)_{,\eta\eta\eta\eta} \\
& +2\lambda^2(\bar{D}_{12}+2\bar{D}_{66})(\;)_{,\eta\eta\xi\xi} + (1/4\pi^2)\bar{D}_{22}(\;)_{,\xi\xi\xi\xi} + 4\pi^2\bar{\rho}(\;)_{,tt}.
\end{aligned} \tag{14}
$$

Here, f is assumed to be expressed as a function of the nondimensional circumferential co-ordinate ξ and a prime denotes ordinary differentiation with respect to ξ. Setting $f(\xi) = 1$ and neglecting all inertia terms, eqns (13) reduce to the Flugge-type equations, given by Cheng and Ho[8], for the stability analysis of anisotropic laminated circular cylindrical shells under combined loading.

Equations (13) and (14) seem to be quite complicated. However, there are many engineering applications for which these equations can be considerably simplified. Thus, in the case of a cross-ply laminated shell (consisting of orthotropic layers whose material axes of symmetry coincide with the curvilinear shell co-ordinates):

$$A_{16} = A_{26} = 0, \quad D_{16} = D_{26} = 0, \quad B_{16} = B_{26} = 0. \tag{15}$$

Furthermore, for a regular antisymmetric cross-ply laminated shell (even number of layers consisting of the same orthotropic material and thickness and with material axes of symmetry alternately oriented at angles 0 and 90° to the shell co-ordinates), it can be shown that:

$$A_{22} = A_{11},\ D_{22} = D_{11}, \quad B_{22} = -B_{11}, \quad B_{12} = B_{66} = 0. \tag{16}$$

For an antisymmetric angle-ply laminated shell (even number of layers of the same thickness and orthotropic material, and with material axes of symmetry alternately oriented at angles of $+\theta$ and $-\theta$ to the shell axis), it can be shown that the first two of the relations (15) are still valid but B_{16} and B_{26} are the only nonzero coupling stiffnesses.

For symmetric laminates (symmetry of both geometry and material properties about the middle surface) all coupling stiffnesses B_{ij} can be shown to be zero. However, this does not necessarily imply that the shell can be considered a homogeneous one. For homogeneous shells, the following additional relationship must be satisfied:

$$D_{ij} = A_{ij}h^2/12 \quad (i, j = 1, 2, 6). \tag{17}$$

Furthermore, in the special case of a homogeneous isotropic shell, extensional stiffnesses are given as follows:

$$A_{11} = A_{22} = hE/(1-\nu^2), \quad A_{12} = hE\nu/(1-\nu^2),$$
$$A_{66} = hE/2(1+\nu), \quad A_{16} = A_{26} = 0,$$

where E and ν are Young's modulus and Poisson's ratio, respectively.

4. APPLICATION FREE VIBRATIONS OF CROSS-PLY LAMINATED NONCIRCULAR CYLINDRICAL SHELLS

It would be of interest to use the derived equations in order to solve a particular problem. Thus, the free vibration problem of a cross-ply laminated noncircular cylindrical shell subjected to the following S2 simply supported edge boundary conditions is considered:

$$N_x = v = w = M_x = 0, \text{ at } \eta = 0,1. \tag{19}$$

As it was mentioned before, because of the relations (15), the Flugge-type eqns (13) and (14) are considerably simplified. Furthermore, for the considered problem, all terms containing the loading parameters $\bar{p}$, $\bar{P}$ and $\bar{T}$, in the expressions (14) must be omitted.

The problem will be solved by the same procedure used by Soldatos and Tzivanidis in Ref. [9]. There, the Donnell-type equations had been used and solved by employing the method of Galerkin. Thus, the shell middle surface displacement components are expanded into the following Fourier-series form:

$$\begin{aligned} u &= \cos(\omega t)\cos(m\pi\eta)\sum_{n=0}^{N} \alpha a_n \cos(2n\pi\xi), \\ v &= \cos(\omega t)\sin(m\pi\eta)\sum_{n=0}^{N} \alpha b_n \sin(2n\pi\xi), \\ w &= \cos(\omega t)\sin(m\pi\eta)\sum_{n=0}^{N} \alpha c_n \cos(2n\pi\xi), \end{aligned} \tag{20}$$

which satisfies the edge boundary conditions and represents symmetric displacements in the circumferential direction (for antisymmetric displacements the sine and cosine functions in the ξ direction must be replaced by cosine and sine functions respectively). In the expansions (20), ω represents a certain unknown natural frequency, m and $2n$ are the axial and circumferential halfwave numbers, a_n, b_n and c_n are unknown constant coefficients and α is equal to 1/2 if $n = 0$ and is equal to 1 if $n > 0$.

In order to solve the free vibration problem of a homogeneous isotropic oval cylindrical shell subjected to S2 edge boundary conditions, Culberson and Boyd [14], introduced the displacement model (20) into Love-type equations of motion and derived $3(N+1)$ recurrence formulas for the $3(N+1)$ unknown constants a_n, b_n and $c_n (n = 0, 1, \ldots, N)$. However, the Fourier-series expansion (20) is a special case of the more general modal expansion used by Chen and Kempner [15] for the investigation of the effect of various types of boundary conditions on the dynamic characteristics of homogeneous isotropic oval cylinders. There, a variational method equivalent to the Ritz's one had been applied onto the energy functional of the Sanders' shell theory [16].

Since there is a very close connection between the two methods of Ritz and Galerkin [17], it seems that the modal expansion method used in Ref. [15] can be also used in conjunction with the Galerkin's method, so that the influence of various types of boundary conditions on the dynamic characteristics of cross-ply laminated noncircular cylindrical shells to be investigated. However, this problem will be treated at a later date. Here, only the free vibration problem of the noncircular shell subjected to S2 edge boundary conditions will be studied.

To this end, introduction of the displacement model (20) into the shell differential equations and application of the method of Galerkin:

$$\int_0^1 [L_{11}(u)+L_{12}(v)+L_{13}(w)]\cos(2i\pi\xi)\,dz=0,$$
$$\int_0^1 [L_{21}(u)+L_{22}(v)+L_{23}(w)]\sin(2i\pi\xi)\,dz=0, \qquad (21)$$
$$\int_0^1 [L_{31}(u)+L_{32}(v)+L_{33}(w)]\cos(2i\pi\xi)\,dz=0, \quad i=0,1,\ldots,N,$$

lead to the following classical algebraic eigenvalue problem:

$$\left(\begin{bmatrix} \mathbf{T}_{11} & \mathbf{T}_{12} & \mathbf{T}_{13} \\ \mathbf{T}_{21} & \mathbf{T}_{22} & \mathbf{T}_{23} \\ \mathbf{T}_{31} & \mathbf{T}_{32} & \mathbf{T}_{33} \end{bmatrix} - \bar{\omega}^2[I]\right)\begin{bmatrix} \mathbf{a} \\ \mathbf{b} \\ \mathbf{c} \end{bmatrix} = [0], \qquad (22)$$

where:

$$\bar{\omega}^2=\bar{\rho}\omega^2. \qquad (23)$$

In eqn (22), $\mathbf{T}_{jk}(j,k=1,3)$ are $(N+1)\times(N+1)$ square matrices. Since $\sin(2n\pi\xi)=0$ for $n=0$, $\mathbf{T}_{12}$ and $\mathbf{T}_{32}$ are $N\times(N+1)$ matrices; since $\sin(2i\pi\xi)=0$ for $i=0$, $\mathbf{T}_{21}$ and $\mathbf{T}_{23}$ are $(N+1)\times N$ matrices and $\mathbf{T}_{22}$ is a $N\times N$ square matrix. Similarly, for antisymmetric displacements $\mathbf{T}_{jk}(j,k=1,3)$ are $N\times N$ square matrices, $\mathbf{T}_{21}$ and $\mathbf{T}_{23}$ are $N\times(N+1)$ matrices, $\mathbf{T}_{12}$ and $\mathbf{T}_{32}$ are $(N+1)\times N$ matrices and $\mathbf{T}_{22}$ is a $(N+1)\times(N+1)$ square matrix. For both cases (symmetric and antisymmetric displacements) the elements of those $\mathbf{T}_{rs}$ matrices $(r,s=1,2,3)$ are given in Appendix B. In eqn (22), **a**, **b** and **c** represent proper column matrices which contain the unknown coefficients a_n, b_n and c_n.

The eigenvalue problem (22), solved by a standard numerical procedure, gives $3N+2$ eigenvalues ($3N+1$ in the case of antisymmetric displacements), each one of which is an approximation of a corresponding natural frequency of the shell. Thus, the integer N must be chosen so that, for the obtained numerical results, convergence be ensured to the desired accuracy.

In the Donnell-type equations used in Ref.[9], only transverse inertia had been considered. Furthermore, in the displacement series expansions, the terms associated with the $n=0$ mode had been omitted. Thus, from the corresponding eigenvalue problem, only N eigenvalues were obtained each one of which was representing a flexural vibration natural frequency of the shell, associated with a particular mode (m,n).

Since in-plane inertias have been retained in this study, three natural frequencies are associated with each mode having $n>0$ and two, a flexural and an axial one, with the $n=0$ mode. For antisymmetric displacements only one natural frequency associated with the $n=0$ mode, the circumferential one, is obtained.

4.1 *The oval cylindrical shell*

For a numerical application, an oval cylindrical shell is considered. According to the oval curvature representation introduced by Romano and Kempner[18,19], the function $f(\xi)$ is determined as follows:

$$f(\xi)=1+\epsilon\cos(4\pi\xi), \qquad (24)$$

where ξ is an eccentricity parameter such that $|\epsilon|\leq 1$. Expression (24) represents a doubly symmetric oval configuration so, as in the case of elliptic shells[20,21], even and odd displacements (n even or odd integer, respectively) are uncoupled each other (see also Appendix B).

Furthermore, changing the sign of ϵ in expression (24), a rotation of the oval arises through 90° or, equivalently, a change, through 90°, of the oval circumferential coordinate origin. As indicated by Fig. 2(a), this change does not affect the even mode shapes ($n=0,2,4,\ldots$) which are symmetric about both axes of the oval (doubly symmetric mode shapes). Thus, by the proposed analysis, symmetric displacements give identical even frequencies for $\pm\epsilon$; also antisymmetric displacements give identical even frequencies for $\pm\epsilon$.

On the other hand, as indicated by Fig. 2(b), the change of the circumferential coordinate origin by 90°, influences the odd mode shapes ($n = 1, 3, 5, \ldots$) which are symmetric about one of the oval axes but antisymmetric about the other one (singly symmetric mode shapes). As a result, odd frequencies obtained for symmetric displacements and $+\epsilon(-\epsilon)$ are identical to the corresponding odd frequencies obtained for antisymmetric displacements and $-\epsilon(+\epsilon)$.

These observations are clearly demonstrated in Table 1, where some of the nondimensional transverse frequencies ω of a two-layered boron-epoxy shell, obtained by both Flugge and Donnell-type theories, are presented. It is, therefore, quite obvious that the amount of the numerical work can be considerably reduced. Thus, all results indicated throughout this paper, except those of Table 1, were obtained for $0 \leq \epsilon \leq 1$.

Finally, for the case of a circular cylindrical shell ($\epsilon = 0$), since a circle is symmetric about any one of its diameters, nothing changes with any change of its circumferential coordinate origin. Consequently, since with a change of this origin by 90° symmetric displacements produce the antisymmetric ones, for a circular cylindrical shell, symmetric and antisymmetric displacements give identical numerical results (see also Appendix B).

4.2 *Numerical results and discussion*

All numerical results obtained were for shells with constant ratio $h/R_0 = 0.01$. Only frequencies associated with $m = 1$ axial half-wave number (the lowest one) had been calculated.

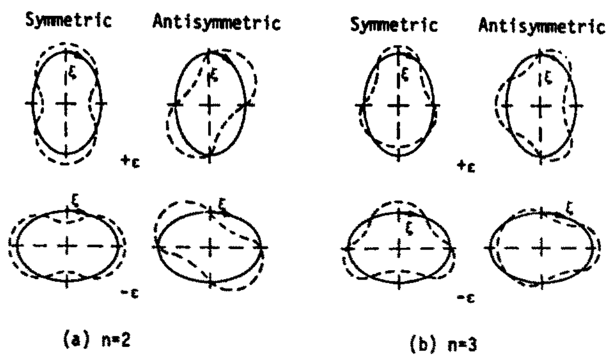

Fig. 2. Mode-shape classifications for flexural displacements of a shell with doubly symmetric cross-sections.

Table 1. Nondimensional flexural vibration frequency parameters $\bar{\omega}$, for a two-layered boron-epoxy shell ($L_x/R_0 = 1$, $|\epsilon| = 0.20$)

	Symmetric Displacements				Antisymmetric Displacements			
	ε = 0.20		ε = -0.20		ε = 0.20		ε = - 0.20	
n	Flugge	Donnell	Flugge	Donnell	Flugge	Donnell	Flugge	Donnell
0	1.01771	1.01880	1.01771	1.01880	-	-	-	-
1	0.63208	0.63297	0.55170	0.55225	0.55170	0.55225	0.63208	0.63297
2	0.38524	0.38593	0.38524	0.38593	0.39243	0.39312	0.39243	0.39312
3	0.27797	0.27866	0.27632	0.27700	0.27632	0.27700	0.27797	0.27866
4	0.21297	0.21379	0.21297	0.21379	0.21272	0.21354	0.21272	0.21354
5	0.17475	0.17587	0.17472	0.17583	0.17472	0.17583	0.17475	0.17587
6	0.14719	0.14831	0.14719	0.14831	0.14717	0.14829	0.14717	0.14829
7	0.14604	0.14732	0.14603	0.14732	0.14603	0.14732	0.14604	0.14732
8	0.16621	0.16797	0.16621	0.16797	0.16620	0.16796	0.16620	0.16796
9	0.18691	0.18881	0.18691	0.18881	0.18691	0.18881	0.18691	0.18881
10	0.21812	0.22001	0.21812	0.22001	0.21812	0.22001	0.21812	0.22001
11	0.25673	0.25859	0.25673	0.25859	0.25673	0.25859	0.25673	0.25859
12	0.30109	0.30291	0.30109	0.30291	0.30109	0.30291	0.30109	0.30291

Furthermore, since there is an infinite complexity of the class of cross-ply laminates, only regular antisymmetric cross-ply laminated shells had been considered, so except of the relations (15), relations (16) are also valid. It can be furthermore shown[22], that the only nonvanishing coupling stiffnesses, B_{11} and B_{22}, are inversely proportional to the shell number of layers. Thus, for this kind of laminated composites, the additional coupling between bending and extension, due to the shell lamination, dies out as the number of layers increases.

For a comparison between Donnell-type[9] and Flugge-type theories, a family of two-layered boron-epoxy shells ($E_1/E_2 = 10$, $G/E_2 = 0.5$, $\nu_{12} = 0.25$) had been used. For a relatively short shell ($L_x/R_0 = 1$) with quite small eccentricity ($|\epsilon| = 0.2$), corresponding nondimensional flexural vibration frequencies, $\bar{\omega}$, obtained by both theories, are cited in Table 1. Obviously, both theories give practically identical results. This is because the shell is quite short and behaves like a quasi-shallow one[23, 24].

However,,as indicated by Tables 2 and 3, where corresponding results are cited for longer shells ($L_x/R_0 = 6$ and 12, respectively) the accuracy of the Donnell shallow shell theory is continually decreased as far as the shell axial length is increased, especially for frequencies

Table 2. Nondimensional flexural vibration frequency poarameters $\bar{\omega}$, for a two-layered boron-epoxy shell ($L_x/R_0 = 6$, $|\epsilon| = 0.20$)

	Symmetric		Antisymmetric	
n	Flugge	Donnell	Flugge	Donnell
n	0.52236	0.52290	-	-
1	0.09937	0.10047	0.09202	0.09100
2	0.04743	0.04687	0.04651	0.04680
3	0.02877	0.02962	0.02866	0.02952
4	0.03408	0.03684	0.03278	0.03427
5	0.04875	0.05067	0.04875	0.05067
6	0.07049	0.07243	0.07049	0.07243
7	0.09678	0.09871	0.09678	0.09871
8	0.12725	0.12916	0.12725	0.12916
9	0.16183	0.16371	0.16183	0.16371
10	0.20049	0.20233	0.20049	0.20233
11	0.24321	0.26440	0.24231	0.26440
12	0.29000	0.30824	0.29000	0.30824

Table 3. Nondimensional flexural vibration frequency parameters $\bar{\omega}$, for a two-layered boron-epoxy shell ($L_x/R_0 = 12$, $|\epsilon| = 0.20$)

	Symmetric		Antisymmetric	
n	Flugge	Donnell	Flugge	Donnell
0	0.26125	0.26152	-	-
1	0.03489	0.03801	0.03708	0.03447
2	0.01846	0.02210	0.01589	0.01552
3	0.01770	0.01837	0.01741	0.01832
4	0.03199	0.03183	0.02952	0.03168
5	0.04786	0.04982	0.04786	0.04982
6	0.07021	0.07216	0.07021	0.07216
7	0.09665	0.09858	0.09665	0.09858
8	0.12716	0.12907	0.12716	0.12907
9	0.16175	0.16363	0.16175	0.16363
10	0.20040	0.20224	0.20040	0.20224
11	0.24311	0.24492	0.24311	0.24492
12	0.28989	0.30814	0.28989	0.30814

with small nominal circumferential wave number n. Let us, for instance, consider the case of the frequencies obtained for symmetric displacements with $n = 1, 2$ and 3. Although for $L_x/R_0 = 6$ the predicted by the Donnell theory frequencies are, respectively, about 1, 1.3 and 3% higher than the corresponding frequencies obtained by the Flugge-type theory, for the shell with $L_x/R_0 = 12$, the corresponding discrepancies are about 8.9, 8.9 and 4%, respectively. Similarly, for the frequencies obtained for antisymmetric displacements with $n = 1, 3$ and 4, although for $L_x/R_0 = 6$ the Donnell's theory predictions are about 1% lower and 2.7 and 4.6% higher, respectively, than the corresponding Flugge's theory ones, for $L_x/R_0 = 12$, the corresponding discrepancies are about 7.5 and 7.5%, respectively.

Furthermore, a comparison between corresponding results, cited in Tables 2 and 4, leads to the conclusion that the eccentricity parameter ϵ is also affecting considerably the accuracy of the Donnell's theory results, especially for frequencies with small nominal circumferential wave numbers. Let us consider, for instance, the case of the fundamental frequency ($n = 3$) obtained for symmetric displacements. For $\epsilon = 0.2$ (Table 2) the fundamental frequency obtained by the Donnell-type theory is about 3% higher than that one obtained by the Flugge-type theory, but for $\epsilon = 1.0$ (Table 4) the Donnell's theory prediction is about 9.3% lower than the corresponding Flugge's theory one.

Further comparisons between corresponding results obtained by both theories but not cited here, have shown that the dependency of the accuracy of the Donnell-type theory upon the eccentricity parameter ϵ is continually increased as far as the shell axial length is increased. However, independently of the value of ϵ, for relatively short ($L_x/R_0 < 1$) two-layered boron-epoxy cylinders, the observed discrepancies, between corresponding results obtained by both theories, were never exceeded the engineering admissible relative error 5%.

A remarkable observation is that, independently of the theory used, the difference of corresponding frequencies obtained for symmetric and antisymmetric displacements becomes less and less observable, provided that their circumferential wave number n is quite high. This is because of the fact that as the number of nodes increases, the radius of curvature within the arc between nodes becomes more or less constant, even though the eccentricity may be large.

When the eccentricity parameter ϵ is small, the nominal circumferential half-wave number n of a frequency is determined simply by one-half of nodes along the oval contour. However, as the eccentricity is increased the mode shapes may be varied significantly from those of the circular cases. Thus, for large values of the eccentricity parameter, n may be determined by the curves tracing the continuous variation of the frequencies versus ϵ. Those curves are indicated in Fig. 3, for a two-layered boron-epoxy shell.

Figure 4 indicates that the orthotropic modulus ratio E_1/E_2 affects considerably the

Table 4. Nondimensional flexural vibration frequency parameters $\bar{\omega}$, for a two-layered boron-epoxy shell ($L_x/R_0 = 6$, $|\epsilon| = 1$)

	Symmetric		Antisymmetric	
n	Flugge	Donnell	Flugge	Donnell
0	0.52254	0.52308	-	-
1	0.10904	0.11394	0.08569	0.07875
2	0.35165	0.35225	0.05751	0.05291
3	0.02814	0.02548	0.01621	0.01541
4	0.04708	0.04448	0.03051	0.02903
5	0.05108	0.05156	0.05206	0.05144
6	0.06931	0.07221	0.06805	0.07221
7	0.09571	0.09828	0.09552	0.09828
8	0.12606	0.12868	0.12607	0.12868
9	0.16057	0.16321	0.16057	0.16321
10	0.19917	0.20183	0.19917	0.20183
11	0.24186	0.24451	0.24186	0.24451
12	0.28862	0.29126	0.28862	0.29126

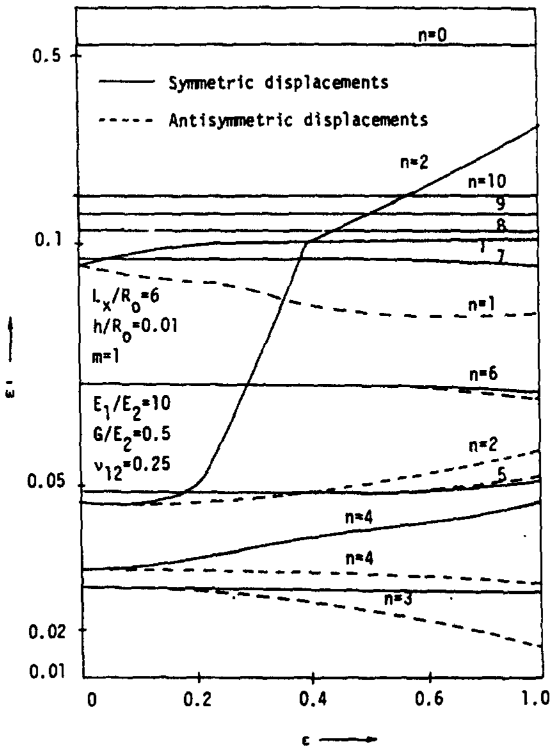

Fig. 3. Variation of flexural vibration frequency parameters versus the oval eccentricity parameter.

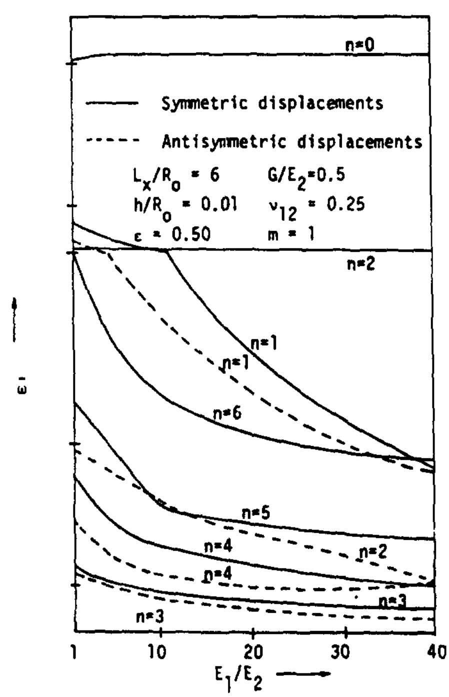

Fig. 4. Variation of flexural vibration frequency parameters versus the orthotropic modulus ratio.

frequencies of a two-layered shell. There, values of G_{12}/E_2 and ν_{12} are fixed because the influence of their variation on the shell frequencies is small compared to that of E_1/E_2. Furthermore, the effect of coupling between bending and extention, due to the shell lamination, on the shell frequencies depends essentially on the orthotropic modulus ratio E_1/E_2, as Fig. 5 indicates. There, the variation of the fundamental frequency ($n = 3$) of an oval shell, having the same geometrical characteristics with that of Fig. 3 and consisting of 2, 4 and infinite number of layers, is indicated.

Obviously, the effect of that lamination coupling between bending and extension is to reduce frequencies from their orthotropic values (∞ number of layers). This reduction is continually increased as far as the orthotropic modulus ratio E_1/E_2 is increased. However, the lamination coupling effect rapidly dies out as the number of layers of the antisymmetric cross-ply laminated shell is increased.

5. CONCLUSIONS

For a generally anisotropic laminated thin elastic non-circular cylindrical shell, subjected to a combined loading, the equations of motion of a second approximation Flugge-type theory have been derived in terms of the shell middle surface displacement components. As an application of the derived equations, the free vibration problem of a cross-ply laminated shell, subjected to S2 simply supported edge boundary conditions, have been solved and numerical results have been presented for oval shells.

From the comparison attempted between corresponding results obtained by both the Flugge-type equations, derived here, and the much simpler Donnell-type ones, available in the literature, it has been shown that, for this particular problem, the quasi-shallow shell equations are accurate enough provided that the shell is short enough. The results of the Donnell-type equations become more and more inaccurate, and therefore the use of the Flugge-type equations is needed, as far as either the axial length of the cylinder or the oval eccentricity parameter is increased.

Apparently, the Flugge-type equations give more accurate results than the quasi-shallow ones and, possibly, the coresponding first approximation equations, because of the inclusion of terms involving z/R in comparison with unity. However, it must be pointed out that, in spite of

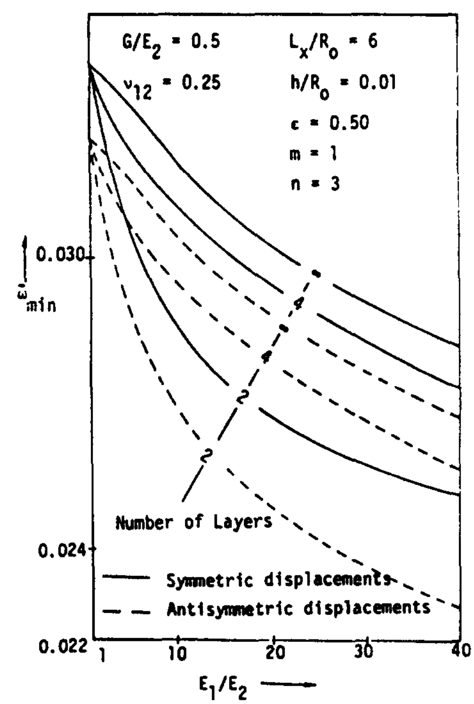

Fig. 5. Variation of flexural vibration fundamental frequency parameters versus the orthotropic modulus ratio and the number of layers.

the inclusion of these terms, the validity of the equations derived here is restricted only in consideration with thin shells. For the analysis of thick shells, the derived equations must be improved so that that transverse shear deformation as well as rotating inertia be taken into consideration.

Acknowledgements—The author wishes to thank the University of Nottingham, England, where the main part of this study was started and completed while he held a visiting Research Fellowship in the Department of Theoretical Mechanics. I also wish to thank the reviewer of the manuscript for his well aimed and very helpful remarks.

REFERENCES

1. L. H. Donnell, Stability of thin-walled tubes under torsion. NACA Rept. 479 (1933).
2. S. B. Dong, K. S. Pister and R. L. Taylor, On the theory of laminated anisotropic shells and plates. *J. Aerospace Sci.* 29, 969 (1962).
3. K. P. Soldatos, Free vibrations of antisymmetric angle-ply laminated circular cylindrical panels. *Quart. J. Mech. Appl. Math.* 36, 207 (1983).
4. A. E. H. Love, *A Treatise on the Mathematical Theory of Elasticity*, 4th Edn. Cambridge University Press (1952).
5. C. W. Bert, J. L. Baker and D. M. Egle, Free vibrations of multilayer anisotropic cylindrical shells. *J. Comp. Mater.* 3, 480 (1969).
6. G. B. Greenberg and Y. Stavsky, Vibrations of laminated filament-wound cylindrical shells. *AIAA J.* 19, 1055 (1981).
7. W. Flugge, *Stresses in Shells*. 2nd Edn. Springer-Verlag, Berlin (1973).
8. S. Cheng and B. P. C. Ho, Stability of heterogeneous aeoltopic cylindrical shells under combined loading. *AIAA J.* 1, 892 (1963).
9. K. P. Soldatos and G. J. Tzivanidis, Buckling and vibration of cross-ply laminated non-circular cylindrical shells. *J. Sound Vib.* 82, 425 (1982).
10. Y. Stavsky and R. Lowey, On vibration of heterogeneous orthotropic cylindrical shells. *J. Sound Vib.* 15, 235 (1971).
11. J. B. Greenberg and Y. Stavsky, Buckling and vibration of orthotropic composite cylindrical shells. *Acta Mechanica* 36, 15 (1980).
12. B. O. Almroth, Influence of edge conditions on the stability of axially compressed cylindrical shells. *AIAA J.* 4, 134 (1966).
13. R. M. Jones, *Mechanics of Composite Materials*. McGraw-Hill, New York (1975).
14. L. Culberson and D. Boyd, Free vibrations of freely supported oval cylinders. *AIAA J.* 9, 1474 (1971).
15. Y. Chen and J. Kempner, Modal method for free vibration of oval cylindrical shells with simply supported or clamped edges. *J. Appl. Mech.* 45, 142 (1978).
16. J. L. Sanders, An improved first approximation theory for thin shells. NASA TR-R24 (1959).
17. L. Kantorovich and V. Krylov, *Approximate Methods in Higher Analysis*. Noordhoff, New York (1964).
18. F. Ramano and J. Kempner, Stress and displacement analysis of a simply supported noncircular cylindrical shell under lateral pressure. Polytechnic Institute of New York, PIBAL Rep. 415 (1958).
19. F. Ramano and J. Kempner, Stresses in short noncircular cylindrical shells under lateral pressure. *J. Appl. Mech.* 29, 669 (1962).
20. J. Sewall and C. Pussey, Vibration study of clamped-free elliptical cylindrical shells *AIAA J.* 9, 1004 (1971).
21. K. Soldatos, C. Massalas and G. Tzivanidis, Dynamic analysis of thin elastic noncircular conical shells. *Acta Mechanica* 46, 207 (1983).
22. S. W. Tsai, Structural behaviour of composite materials. NASA CR-71 (1964).
23. H. Kraus, *Thin Elastic Shells*. Wiley, New York (1967).
24. D. O. Brush and B. O. Almroth, *Buckling of Bars, Plates and Shells*. McGraw-Hill, New York (1975).

APPENDIX A

The stiffness submatrices appearing in eqns (6)

The stiffness submatrices appearing in eqns (6) are given, in terms of the extensional, coupling and bending submatrices components defined in eqn (8), as follows:

$$[A'] = \begin{bmatrix} A_{11}+B_{11}/R & A_{12}+B_{12}/R & A_{16}+B_{16}/R+D_{16}/2R^2 \\ A_{12} & A_{22} & A_{26}+D_{26}/2R^2 \\ A_{16}+B_{16}/R & A_{26}+B_{26}/R & A_{66}+B_{66}/R+D_{66}/2R^2 \\ A_{16} & A_{26} & A_{66}+D_{66}/2R^2 \end{bmatrix}. \tag{A1}$$

$$[B'] = \begin{bmatrix} B_{11}+D_{11}/R & B_{12} & B_{16}+D_{16}/2R \\ B_{12} & B_{22}-D_{22}/R & B_{26}-D_{26}/2R \\ B_{16}+D_{16}/R & B_{26} & B_{66}+D_{66}/2R \\ B_{16} & B_{26}-D_{26}/R & B_{66}-D_{66}/2R \end{bmatrix}. \tag{A2}$$

$$[C'] = \begin{bmatrix} B_{11}+D_{11}/R & B_{12}+D_{12}/R & B_{16}+D_{16}/R \\ B_{12} & B_{22} & B_{26} \\ B_{16}+D_{16}/R & B_{26}+D_{26}/R & B_{66}+D_{66}/R \\ B_{16} & B_{26} & B_{66} \end{bmatrix}. \tag{A3}$$

APPENDIX B

The matrices appearing in eqn (22)

The elements of the matrices $T_{rs}(r, s = 1, 2, 3)$ appearing in eqn (22) are given as follows:

$$
\begin{aligned}
(T_{11})_{in} &= (\lambda_m^2 + n^2\bar{A}_{66})\delta_{ni} + 2[(\lambda_m^2\bar{B}_{11} - n^2\bar{B}_{66})\theta_1(n,i) + n^2\bar{D}_{66}\theta_2(n,i)] - \mu_s(n/\pi)[\bar{B}_{66}\theta_3(n,i) - 2\bar{D}_{66}\theta_4(n,i)],\\
(T_{12})_{in} &= -\mu_s\lambda_m n[(\bar{A}_{12} + \bar{A}_{66})\delta_{ni} + 2(\bar{B}_{12} + \bar{B}_{66})\theta_1(n,i)] - (\lambda_m/2\pi^2)\bar{B}_{66}\theta_3(n,i),\\
(T_{13})_{in} &= (T_{31})_{in} = -2\lambda_m(\bar{A}_{12} + \lambda_m^2\bar{D}_{11} - n^2\bar{D}_{66})\theta_1(n,i) - \lambda_m[\lambda_m^2\bar{B}_{11} + n^2(\bar{B}_{12} + 2\bar{B}_{66})]\delta_{ni} + \mu_s(\lambda_m n/\pi^2)\bar{D}_{66}\theta_3(n,i),\\
(T_{21})_{in} &= -\mu_s\lambda_m n[(\bar{A}_{12} + \bar{A}_{66})\delta_{ni} + 2(\bar{B}_{12} + \bar{B}_{66})\theta_5(n,i)],\\
(T_{22})_{in} &= (\lambda_m^2\bar{A}_{66} + n^2\bar{A}_{22})\delta_{ni} + 2(3\lambda_m^2\bar{B}_{66} + n^2\bar{B}_{22})\theta_5(n,i) + 6\lambda_m^2\bar{D}_{66}\theta_6(n,i),\\
(T_{23})_{in} &= \mu_s n[n^2\bar{B}_{22} + \lambda_m^2(\bar{B}_{12} + 2\bar{B}_{66})]\delta_{ni} + \mu_s 2n[\bar{A}_{22} + \lambda_m^2(\bar{D}_{12} + 3\bar{D}_{66})]\theta_5(n,i) - (1/\pi)\bar{A}_{22}\theta_7(n,i)\\
&\quad - \mu_s 2n^3\bar{D}_{22}\theta_8(n,i) + 2\bar{B}_{22}[-\mu_s n\theta_9(n,i) + (1/2\pi)\theta_{10}(n,i)] - 2\bar{D}_{22}[-\mu_s n\theta_{11}(n,i) + (1/\pi)\theta_{12}(n,i)],\\
(T_{32})_{in} &= \mu_s n[n^2\bar{B}_{22} + \lambda_m^2(\bar{B}_{12} + 2\bar{B}_{66})]\delta_{ni} + \mu_s 2n[\bar{A}_{22} + \lambda_m^2(\bar{D}_{12} - 3\bar{D}_{66})]\theta_1(n,i),\\
(T_{33})_{in} &= [\lambda_m^4\bar{D}_{11} + 2\lambda_m^2 n^2(\bar{D}_{12} + 2\bar{D}_{66}) + n^4 D_{22}]\delta_{ni} + 2(\bar{A}_{22} - 2n^2\bar{D}_{22})\theta_2(n,i) + 4(\lambda_m^2\bar{B}_{12} + n^2\bar{B}_{22})\theta_1(n,i)\\
&\quad + 2\bar{B}_{22}[\mu_s(n/\pi)\theta_3(n,i) - \theta_{13}(n,i)] + 2\bar{D}_{22}[\theta_{14}(n,i) - \mu_s\theta_4(n,i)],\quad n, i = 0, 1, 2, \ldots N,
\end{aligned}
\tag{B1}
$$

where $\lambda_m = \lambda m\pi$, δ_{ni} is the Kronecker's delta and $\mu_s = 1$ or -1 for symmetric or antisymmetric displacements, respectively.

For symmetric displacements, the quantites $\theta_j(n, i)$ $(j = 1, 2, \ldots, 14)$ are given, in integral form as follows:

$$
\begin{aligned}
\theta_1(n,i) &= \alpha\int_0^1 f(\xi)\cos(2n\pi\xi)\cos(2i\pi\xi)\,d\xi,\\
\theta_2(n,i) &= \alpha\int_0^1 f^2(\xi)\cos(2n\pi\xi)\cos(2i\pi\xi)\,d\xi,\\
\theta_3(n,i) &= \alpha\int_0^1 \frac{df}{d\xi}\sin(2n\pi\xi)\cos(2i\pi\xi)\,d\xi,\\
\theta_4(n,i) &= \alpha\int_0^1 f(\xi)\frac{df}{d\xi}\sin(2n\pi\xi)\cos(2i\pi\xi)\,d\xi,\\
\theta_5(n,i) &= \alpha\int_0^1 f(\xi)\sin(2n\pi\xi)\sin(2i\pi\xi)\,d\xi,\\
\theta_6(n,i) &= \alpha\int_0^1 f^2(\xi)\sin(2n\pi\xi)\sin(2i\pi\xi)\,d\xi,\\
\theta_7(n,i) &= \alpha\int_0^1 \frac{df}{d\xi}\cos(2n\pi\xi)\sin(2i\pi\xi)\,d\xi,\\
\theta_8(n,i) &= \alpha\int_0^1 \frac{df}{d\xi}\sin(2n\pi\xi)\sin(2i\pi\xi)\,d\xi,\\
\theta_9(n,i) &= \alpha\int_0^1 f(\xi)\frac{df}{d\xi}\sin(2n\pi\xi)\sin(2i\pi\xi)\,d\xi,\\
\theta_{10}(n,i) &= \alpha\int_0^1 \left(\frac{df}{d\xi}\right)^2\cos(2n\pi\xi)\sin(2i\pi\xi)\,d\xi,\\
\theta_{11}(n,i) &= \alpha\int_0^1 \frac{df}{d\xi}f^2(\xi)\sin(2n\pi\xi)\sin(2i\pi\xi)\,d\xi,\\
\theta_{12}(n,i) &= \alpha\int_0^1 f(\xi)\left(\frac{df}{d\xi}\right)^2\cos(2n\pi\xi)\sin(2i\pi\xi)\,d\xi,\\
\theta_{13}(n,i) &= \alpha\int_0^1 \left[f^3(\xi) + (1/4\pi^2)\frac{d^2f}{d\xi^2}\right]\cos(2n\pi\xi)\cos(2i\pi\xi)\,d\xi,\\
\theta_{14}(n,i) &= \alpha\int_0^1 \left[f^4(\xi) + (1/2\pi^2)\left(\frac{df}{d\xi}\right)^2 + (1/2\pi)^2\frac{d^2f}{d\xi^2}f(\xi)\right]\cos(2n\pi\xi)\cos(2i\pi\xi)\,d\xi.
\end{aligned}
\tag{B2}
$$

Furthermore, if $i = 0$ the elements $(T_{2j})_{in}$ and if $n = 0$ the elements $(T_{j2})_{in}$ $(j = 1, 2, 3)$ must be omitted in the construction of the corresponding matrices.

For antisymmetric displacements, the sine and cosine functions appearing in the expressions (B2) must be replaced by cosine and sine functions, respectively. Furthermore, for $i = 0$ and for $n = 0$ all elements $(T_{kj})_{in}$ and $(T_{jk})_{in}$ $(k = 1, 3;$ $j = 1, 2, 3)$, respectively, must be omitted in the construction of the corresponding matrices.

In any case in which $f(\xi)$ is a very complicated function of the circumferential coordinate ξ, the quantities $\theta_j(n, i)$ $(j = 1, 2, \ldots, 14)$ can be evaluated numerically. However, in the case of the oval shell, the simplicity of the expression (24) permits the quantities $\theta_j(n, i)$ to be evaluated analytically. To this end, the following functions are defined:

$$Z_1(l, n, i) = \alpha \int_0^1 \cos(2l\pi\xi)\cos(2n\pi\xi)\cos(2i\pi\xi)\,\mathrm{d}z = \begin{cases} 1/2\delta_{ni} & l = 0 \\ 1/4 & l \neq 0,\ n + i = l \\ 1/4, & l \neq 0,\ |n - i| = l \\ 0 & \text{otherwise} \end{cases}$$

$$Z_2(l, n, i) = \alpha \int_0^1 \cos(2l\pi\xi)\sin(2n\pi\xi)\sin(2i\pi\xi)\,\mathrm{d}z = \begin{cases} 1/2\delta_{ni} & l = 0,\ n \neq 0 \\ 1/4 & l \neq 0,\ n + i = l \\ 1/4, & l \neq 0,\ |n - i| = l \\ 0. & \text{otherwise} \end{cases} \tag{B3}$$

where l, n and i represent nonegative integers. Then, the quantities $\theta_j(n, i)$ can be expressed as folows:

$$\begin{aligned}
\theta_1(n, i) &= 1/2\delta_{ni} + \epsilon\begin{bmatrix} Z_1(2, n, i) \\ Z_2(2, n, i) \end{bmatrix}, \\
\theta_2(n, i) &= 1/2(1 + \epsilon^2/2)\delta_{ni} + 2\epsilon\begin{bmatrix} Z_1(2, n, i) \\ Z_2(2, n, i) \end{bmatrix} + (\epsilon^2/2)\begin{bmatrix} Z_1(4, n, i) \\ Z_2(4, n, i) \end{bmatrix}, \\
\theta_3(n, i) &= -4\pi\epsilon\begin{bmatrix} Z_2(i, n, 2) \\ Z_2(n, i, 2) \end{bmatrix}, \\
\theta_4(n, i) &= -4\pi\epsilon\begin{bmatrix} Z_2(i, n, 2) \\ Z_2(n, i, 2) \end{bmatrix} - 2\pi\epsilon^2\begin{bmatrix} Z_2(i, n, 4) \\ Z_2(n, i, 4) \end{bmatrix}, \\
\theta_5(n, i) &= 1/2\delta_{ni} + \epsilon\begin{bmatrix} Z_2(2, n, i) \\ Z_1(2, n, i) \end{bmatrix}, \\
\theta_6(n, i) &= 1/2(1 + \epsilon^2/2)\delta_{ni} + 2\epsilon\begin{bmatrix} Z_2(2, n, i) \\ Z_1(2, n, i) \end{bmatrix} + (\epsilon^2/2)\begin{bmatrix} Z_2(4, n, i) \\ Z_1(4, n, i) \end{bmatrix}, \\
\theta_7(n, i) &= -4\pi\epsilon\begin{bmatrix} Z_2(n, i, 2) \\ Z_2(i, n, 2) \end{bmatrix}, \\
\theta_8(n, i) &= \theta_9(n, i) = \theta_{10}(n, i) = \theta_{11}(n, i) = \theta_{12}(n, i) = 0, \\
\theta_{13}(n, i) &= 1/2(1 + 3\epsilon^2/2)\delta_{ni} - \epsilon(1 - 3\epsilon^2/4)\begin{bmatrix} Z_1(2, n, i) \\ Z_2(2, n, i) \end{bmatrix} + (3\epsilon^2/2)\begin{bmatrix} Z_1(4, n, i) \\ Z_2(4, n, i) \end{bmatrix} + (\epsilon^3/4)\begin{bmatrix} Z_1(6, n, i) \\ Z_2(6, n, i) \end{bmatrix}, \\
\theta_{14}(n, i) &= 1/2(1 + 3\epsilon^2 + 3\epsilon^4/8)\delta_{ni} - \epsilon(4 - 3\epsilon^2)\begin{bmatrix} Z_1(2, n, i) \\ Z_2(2, n, i) \end{bmatrix} \\
&\quad - \epsilon^2(5 - \epsilon^2/2)\begin{bmatrix} Z_1(4, n, i) \\ Z_2(4, n, i) \end{bmatrix} + \epsilon^3\begin{bmatrix} Z_1(6, n, i) \\ Z_2(6, n, i) \end{bmatrix} + (\epsilon^4/8)\begin{bmatrix} Z_1(8, n, i) \\ Z_2(8, n, i) \end{bmatrix},
\end{aligned} \tag{B4}$$

where the upper and the lower functions appearing in the braces represent symmetric and antisymmetric displacements respectively.

An attentive observation of the expressions (B4) makes apparent that each one of the functions Z_1 and Z_2, appearing there, has a nonzero contribution only if both n and i are or even or odd integers. As a result, even the odd displacements (n even or odd integer, respectively) are uncoupled and do not affect each other.

It must be also noted that for $\epsilon = 0$ (circular cylindrical shell), the choice of symmetric or antisymmetric displacements does not affect the final value of each one of the quantities $\theta_j(n, i)$. Thus, for a circular cylindrical shell, symmetric and antisymmetric displacements give identical numerical results.